Kinetics of Ion−Molecule Reactions with Dimethyl Methylphosphonate at 298 K for Chemical Ionization Mass Spectrometry Detection of GX

Anthony J. Midey,† Thomas M. Miller,† and A. A. Viggiano*

Air Force Research Laboratory, Space Vehicles Directorate, 29 Randolph Road, Hanscom AFB, Massachusetts 01731-3010

Received: January 20, 2009; Revised Manuscript Received: March 9, 2009

Kinetics studies of a variety of positive and negative ions reacting with the GX surrogate, dimethyl methylphosphonate (DMMP), were performed. All protonated species reacted rapidly, that is, at the collision limit. The protonated reactant ions created from neutrals with proton affinities (PAs) less than or equal to the PA for ammonia reacted exclusively by nondissociative proton transfer. Hydrated H_3O^+ ions also reacted rapidly by proton transfer, with 25% of the products from the second hydrate, $H_3O^+(H_2O)_2$, forming the hydrated form of protonated DMMP. Both methylamine and triethylamine reacted exclusively by clustering. NO^+ also clustered with DMMP at about 70% of the collision rate constant. O^+ and O_2^+ formed a variety of products in reactions with DMMP, with O_2^+ forming the nondissociative charge transfer product about 50% of the time. On the other hand, many negative ions were less reactive, particularly, SF_5^-, SF_6^-, CO_3^-, and NO_3^-. However, F^-, O^-, and O_2^- all reacted rapidly to generate $m/z = 109$ amu anions ($PO_3C_2H_6^-$). In addition, product ions with $m/z = 122$ amu from H_2^+ loss to form H_2O were the dominant ions produced in the O^- reaction. NO_2^- underwent a slow association reaction with DMMP at 0.4 Torr. G3(MP2) calculations of the ion energetics properties of DMMP, sarin, and soman were also performed. The calculated ionization potentials, proton affinities, and fluoride affinities were consistent with the trends in the measured kinetics and product ion branching ratios. The experimental results coupled with the calculated ion energetics helped to predict which ion chemistry would be most useful for trace detection of the actual chemical agents.

Introduction

Detection of chemical weapon agents (CWAs) in the gas phase remains an important problem in many areas such as homeland security and chemical weapon disposal facilities. The analytical requirements are rigorous given the minute quantities needed to cause harm to humans. Chemical weapons disposal and stockpile facilities have some of the most strenuous requirements because the live agents are handled regularly. A recent National Academy of Sciences (NAS) report[1] on monitoring air at chemical agent disposal facilities has examined the need for real-time detection in the plants and concluded that the only current technology that demonstrated enough promise to pursue in the short term is chemical ionization mass spectrometry (CIMS). CIMS has already proven successful at selective and sensitive detection of trace concentrations of many atmospheric neutrals.[2−9] Using the CIMS technique with CWAs will require a search for readily generated primary ions that can react rapidly with the agents and yield product ions with unique mass signatures. The latter goal typically employs ion−molecule reactions that keep the neutral reagent structure intact after ionization.

As chemical weapons cannot be readily studied in most laboratories, the use of surrogates and theoretical calculations is required. This approach has recently been employed in our laboratory to find CIMS reaction schemes for mustard (HD) using the surrogate, 2-chloroethyl ethyl sulfide (2-CEES).[10] Dimethyl methylphosphonate (DMMP), given as $H_3CP(O)(OCH_3)_2$, is a commonly used surrogate for the GX series CWAs, as well as a prototypical organophosphorus and phosphonate ester compound. Cooks and co-workers have studied ionizing DMMP with electron impact (EI) using ion−molecule reactions of two major EI fragments at $m/z = 109$ amu ($C_2H_6PO_3^+$) and 93 amu ($C_2H_6PO_2^+$)[11] as a way to generate fingerprint ions for selective detection. Proton-bound cluster reactions with DMMP have also been studied using proton transfer reactions in ion mobility spectrometers (IMS),[12−17] including bracketing studies to measure the proton affinity (PA) of DMMP.[14] Lum and Grabowski have studied negative ion reactions with DMMP in a flowing afterglow to compare the reactivity of the P−O and C−O bonds,[18] while Johnsen and co-workers have examined the reactions of several air plasma cations with DMMP in a selected ion flow drift tube (SIFDT).[19]

CIMS detection of CWAs benefits from not having to pretreat the gas sample to be analyzed, only requiring the production of easily generated reactant ions that have both large rate constants and unique product ion distributions upon reaction with CWAs to achieve sensitive and selective detection. To find new ion−molecule reactions that meet these two criteria for the GX series agents, a study of experimental rate constants and product ion branching ratios has been conducted using a selected ion flow tube (SIFT) at 298 K for a variety of positive and negative ions reacting with the GX structural surrogate, DMMP. Its structure is shown in Figure 1 along with the structures of sarin (GB) and soman (GD). Most of the functional groups found in the live agent are present in the surrogate compound. Assuming that the P−O−R groups have similar reactivity for different R substituents, the lone difference is then the P−F bond in the CWAs.

* Corresponding author. E-mail: afrl.rvb.pa@hanscom.af.mil.
† Under contract to the Institute for Scientific Research, Boston College, Chestnut Hill, MA.

10.1021/jp900614a CCC: $40.75
Published on Web 04/03/2009

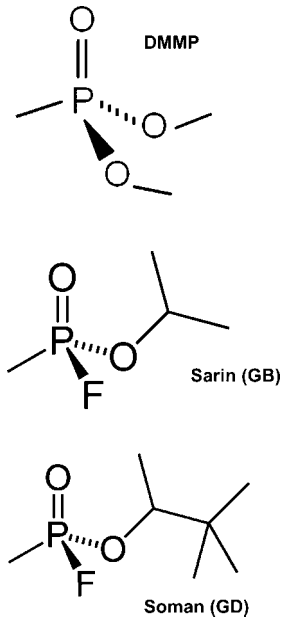

Figure 1. Example drawings of the structures for dimethyl methylphosphonate (DMMP), sarin (GB), and soman (GD) adapted from the NIST Webbook. Structures for all three molecules have been optimized at the MP2(Full)/6-31G(d) level of theory as part of G3(MP2) calculations (not shown).

The reactant ions chosen for this study reflect the typical ions employed in the various atmospheric CIMS instruments,[2−9] that is, SF_6^-, SF_5^-, CO_3^-, and O_2^-, along with the additional ions NO_3^-, NO_2^-, O^-, and F^-. We have also studied the cations used in commercial ion reactors,[20] that is, H_3O^+, O_2^+, and NO^+, as well as other ions chosen to expand upon the previous literature studies of the ion−molecule chemistry of DMMP discussed above, such as O^+ and the first two proton hydrates $H_3O^+(H_2O)_{1-2}$. The latter ions are especially important given that field instruments will be operating in humid air. A series of protonated neutrals with a wide range of PAs (NH_4^+, $CH_3NH_3^+$, $(C_2H_5)_3NH^+$, and $(CH_3)_2COH^+$) have also been investigated to bracket the theoretical values as described below.

In addition, theoretical calculations of the PAs, ionization potentials (IP), and fluoride affinities (FA) of DMMP, sarin, and soman have been performed to augment the studies involving the surrogate. The combination of theory and experiment allows us to predict which of the ions that sensitively and selectively detect DMMP can also be employed to detect the CWAs. The viability of this approach for GX agents has been confirmed by recent sarin (GB) data[21,22] and has also been previously demonstrated for mustard (HD).[10,22]

Experimental Methods

The rate constants and product ion branching ratios were measured at 298 K using the selected ion flow tube (SIFT) at the Air Force Research Laboratory. This instrument was described in detail elsewhere.[23] Therefore, only a brief description follows as related to the current measurements.

The reactant ions were generated in a moderate-pressure source using electron impact ionization. A thoriated iridium filament was used for most of the studies; however, a rhenium metal filament was alternatively used with the halogenated source chemicals. A single reactant ion was selected with a quadrupole mass filter, and it was injected into a fast flow of helium buffer gas that entered the tube through a Venturi inlet. A dilute mixture of ~0.1% DMMP in helium was introduced into the reaction region of the flow tube through a stainless steel inlet 59 cm upstream from a sampling nose cone aperture. The room temperature vapor pressure of DMMP of ~1 Torr was sufficient for conducting the experiments using gas mixtures as the SIFT technique was sensitive to rate constants as low as 1×10^{-11} cm^3 s^{-1}, even with such low reagent concentrations. As the CIMS method requires fast reactions, this lower limit was acceptable, precluding the need for heated inlet lines and more difficult calibrations. After sampling the ions, the product ions and any remaining reactant ions were analyzed using a second quadrupole mass analyzer, with subsequent detection by a conversion dynode multiplier.

The rate constants were obtained by measuring the pseudo first-order decay of the reactant ion as a function of DMMP concentration over a previously measured reaction time. The rate constants have relative uncertainties of ±15% and absolute uncertainties of ±25%.[23] Product ion branching ratios were obtained by plotting the fraction of each product ion versus DMMP concentration, then extrapolating to zero concentration. The extrapolation minimized potential contributions from secondary reactions of the product ions with the DMMP in the flow tube. For the major product ions observed, product branching ratios typically had ±10% uncertainties,[23] including for the cluster ion reactions. The minor product species observed were also reported, despite the possible interference of trace impurities. However, the emphasis of the current experiments was finding the major ionic species that could comprise a chemical fingerprint for use in future CIMS work.[10]

Materials

The following reagents were used in the measurements: dimethyl methylphosphonate (Aldrich, 98%), helium (AGA, 99.997%), oxygen (AGA, 99.999%), nitric oxide (Matheson, 99.5%), nitrogen dioxide (AGA, 99.5%), carbon dioxide (Middlesex Gases, 99.999%), sulfur hexafluoride (Matheson, 99.8%), ammonia (Matheson, 99.99%), acetone (Baker, HPLC grade), monomethylamine (Matheson, 99.5%), triethylamine (Aldrich, ≥99%), and distilled water. All of the reactant ions listed in Tables 1 and 2 were produced using the pure source gases. The materials were used as obtained from the manufacturer, except for performing freeze−pump−thaw treatments on all of the liquid samples, including the DMMP, to remove trapped gases.

Theoretical Methods

To extrapolate from the experimental results for the DMMP surrogate to the GX agents, theoretical calculations of minimum energy structures and energetics have been performed at the G3(MP2) level of theory[24] using Gaussian 03[25] for neutral DMMP, sarin, and soman and their corresponding ionic products for proton, fluoride, oxide, and electron transfer reactions, summarized in Table 3. Calculations of both the oxide affinity (OA) and the electron affinity (EA) for attaching an O^- and e^-, respectively, give negative values for both DMMP and the GX agents; thus, these reaction mechanisms are not discussed further. An average absolute deviation of ±5.4 kJ mol^{-1} is found for energies calculated using G3(MP2) methods.[24] This approach was analogous to our recent work with mustard surrogate 2-CEES.[10]

The goal of the experiments was to find fingerprint product ions for the reaction of various types of ions with the surrogate to extrapolate to reactions with the GX agents. Thus, structure calculations were performed to find energetically allowed pathways for the observed fragment ions to gain some insight

TABLE 1: Rate Constants for the Reaction of Various Positive Ions with Dimethyl Methylphosphonate (DMMP) at 298 K Measured in a Selected Ion Flow Tube (SIFT)[a]

Ion	Products DMMP $H_3CP(O)(OCH_3)_2$	PA[a] kJ mol^{-1}	k 10^{-9} cm^3 s^{-1}	k_{col} 10^{-9} cm^3 s^{-1}
H_3O^+	$[H_3CP(O)(OCH_3)_2]H^+ + H_2O + 207$	691	4.8	4.9
$H_3O^+(H_2O)$	$[H_3CP(O)(OCH_3)_2]H^+ + 2\ H_2O + 71$		3.6	3.8
$H_3O^+(H_2O)_2$	$[H_3CP(O)(OCH_3)_2]H^+ + 3\ H_2O$ - 13 [0.73] $[H_3CP(O)(OCH_3)_2{\bullet}H_2O]H^+ + 2\ H_2O + 45$ [0.27]		3.6	3.2
$(CH_3)_2COH^+$	$[H_3CP(O)(OCH_3)_2]H^+ + (CH_3)_2CO + 86$	812	4.2	3.2
NH_4^+	$[H_3CP(O)(OCH_3)_2]H^+ + NH_3 + 45$	853	4.4	5.5
$CH_3NH_3^+$	$[H_3CP(O)(OCH_3)_2{\bullet}CH_3NH_2]H^+$ - 1	899	5.1	4.0
$(C_2H_5)_3NH^+$	$[H_3CP(O)(OCH_3)_2){\bullet}(C_2H_5)_3N]H^+$ - 51	949	2.9	2.7
		IP (eV)[a]		
NO^+	$[H_3CP(O)(OCH_3)_2{\bullet}NO]^+$	9.26	2.8	4.1
O_2^+	$OP(O)(OCH_3)_2^+ + (CH_3O) + 180$ [0.01] $H_3CP(O)(OCH_3)_2^+ + O_2 + 151$ [0.48] $P(O)(OCH_3)_2^+ + (CH_3 + O_2) + 88$ } [<0.01] $H_2CPO_4^+ + (C_2H_5 + H_2O) + 63$ } $OP(O)(OCH_3)^+ + (CH_3OOCH_3) + 283$ } [0.48] $HP(OCH_3)_2^+ + (CH_2O + O_2) + 65$ $H_3CPH(O)(OCH_3)^+ + (CH_2O + O_2) + 44$ $H_3CP(OH)(OCH_3)^+ + (CH_2O + O_2) + 175$ } $HOPOCH_3^+ + (CH_2O + CH_3 + O_2) + 10$ } [<0.01] $HOPOCH_3^+ + (CH_2O + CH_3O_2) + 146$ $HP(O)(OCH_3)^+ + (CH_3O_2 + CH_2O) + 34$ } $PO_2^+ + (CH_3O + HOC_2H_4OH) - 30$ [<0.01] $PO^+ + (CH_3O_2 + HOC_2H_4OH)$ - 52 [<0.01]	12.1	4.7	4.0
O^+	$OP(O)(OCH_3)_2^+ + CH_3 + 423$ [0.05] $P(O)(OCH_3)_2^+ + (CH_3 + O) + 211$ } [0.14] $H_3CP(O)O(OCH_3) + (CH_3O) + 299$ $H_2CPO_4^+ + (CH_3 + CH_4) + 239$ $H_2CPO_4^+ + (C_2H_5 + H_2) + 192$ } $OP(O)(OCH_3)^+ + (CH_3 + CH_3O) + 102$ } [0.30] $HP(OCH_3)_2^+ + (CH_2O + O) + 189$ $H_3CP(O)H(OCH_3)^+ + (CH_2O + O) + 168$ $H_3CP(OH)(OCH_3)^+ + (CH_2O + O) + 299$ } $CH_2PO_3^+ + (CH_3OH + CH_3) + 60$ } [0.07] $H_3CP(O)OCH_3^+ + (CH_3O + O) + 160$ $P(OCH_3)_2^+ + (CH_3O + O) + 133$ } $HOPOCH_3^+ + (CH_2O + CH_3 + O) + 134$ } [0.44] $HP(O)OCH_3^+ + (CH_2O + CH_3 + O) + 22$ }	13.6	4.2	5.3

[a] The experimental rate constants, k, and the corresponding Su−Chesnavich collision rate constants (k_{col}) are given in units of $\times 10^{-9}$ cm^3 s^{-1}. Product ion branching ratios are given in brackets for reactions with more than one channel. Reaction enthalpies at 298 K in kJ mol^{-1} calculated using G3(MP2) theory are shown with the products. Proton affinity (PA) in kJ mol^{-1} or ionization potential (IP) in eV for the neutral precursor of the reactant ion obtained from the NIST Webbook[34] are also shown.

into the possible reaction pathways. As with the ion−molecule chemistry of 2-CEES,[10] barriers on the potential surfaces would influence the observed product ion branching ratios. However, a complete understanding of the reaction dynamics was beyond the scope of the current work.

Results

Tables 1 and 2 give the measured rate constants and product ion branching ratios for the survey of positive and negative ions, respectively. The measured rate constants are given along with the collision rate constant determined using the Su−Chesnavich parametrized form.[26,27] A literature value[15] of the polarizability for DMMP of 9.9 Å^3 is in good agreement with the estimated value of 10.25 Å^3 calculated using the additivity methods of Miller[28] and of Bosque and Sales.[29] However, a wide discrepancy in the value for the dipole moment of DMMP has been found. Values of 2.86 and 3.62 D have been given by Ewing et al.[16] and Kosolapoff,[30] while the dipole moment taken from the MP2(Full)/6-31G(d) geometry optimization step of the G3(MP2) calculations is much higher at 4.8 D. Different conformers of the neutral DMMP have been found in the infrared spectra of DMMP in low-temperature matrices[31] that will have widely varying dipole moments depending on the structure.[32] MP2 dipole moments tend to be as much as 0.5 D higher than experimental values, with an average deviation of about 0.3 D.[33] Therefore, using the values given above, an average polarizability of 10.1 Å^3 and an average dipole moment of 3.76 D have been used to calculate the collision rate constants.

a. Positive Ion Reactions. All of the positive ions chosen for this study react rapidly with DMMP, satisfying one of the criteria for a good CIMS reagent ion, that is, sensitivity. For the positive ion reactions in Table 1, the literature value for the relevant PA or IP of the neutral precursor for the corresponding reactant ion is listed as well.[34] The measured rate constants approach the collision rate constant, k_{col}, within the combined uncertainties of the two values, particularly considering the large uncertainty in the dipole moment used to calculate k_{col}. Many positive ion chemical ionization schemes rely on either proton or electron transfer, and most of the ions presently studied react accordingly. The current experimental results also provide limits for the ion energetic properties of DMMP that can be compared to the calculated values.

TABLE 2: Rate Constants for the Reaction of Various Negative Ions with Dimethyl Methylphosphonate (DMMP) at 298 K Measured in a Selected Ion Flow Tube (SIFT)[a]

Ion	Products DMMP $H_3CPO(OCH_3)_2$	k 10^{-9} cm^3 s^{-1}	k_{col} 10^{-9} cm^3 s^{-1}
F^-	$P(O)(OCH_3)_2^-$ + CH_3F - 26 [0.85] $H_3CP(O)O(OCH_3)^-$ + CH_3F +154 $(H_3CO)(F)P(O)CH_2^-$ + CH_3OH + 79 [0.15]	3.7	4.9
SF_5^-	No Reaction	<0.01	2.5
SF_6^-	No Reaction	<0.01	2.5
CO_3^-	No Reaction	<0.01	3.2
NO_2^-	$[H_3CPO(OCH_3)_2)\cdot NO_2]^-$	0.013	3.5
NO_3^-	No Reaction	<0.01	3.1
O^-	$H_2CP(O)(OCH_3)OCH_2^-$ + H_2O + 155 [0.82] $H_3CP(O)(OCH_2)_2^-$ + H_2O + 52 $H_3CP(O)(OCH_3)OCH^-$ + H_2O + 104 $HCP(O)(OCH_3)_2^-$ + H_2O + 122 $P(O)(OCH_3)_2^-$ + (CH_3O) + 87 [0.18] $H_3CP(O)O(OCH_3)^-$ + (CH_3O) + 266	6.0	5.3
O_2^-	$P(O)(OCH_3)_2^-$ + (CH_2O+OH) + 37 [0.98] $H_3CP(O)O(OCH_3)^-$ + (CH_3O_2) + 124 $[H_3CP(O)(OCH_3)_2\cdot O_2]^-$ [0.02]	3.6	4.0

[a] The experimental rate constants, k, and the corresponding Su−Chesnavich collision rate constants (k_{col}) are given in units of $\times 10^{-9}$ cm^3 s^{-1}. Product ion branching ratios are given in brackets for reactions with more than one channel. Reaction enthalpies at 298 K calculated using G3(MP2) theory for all mechanisms excluding association are shown along with the products in units of kJ mol^{-1}.

TABLE 3: Various Energetics Results from G3(MP2) Calculations for Dimethyl Methylphosphonate (DMMP), Sarin (GB), and Soman (GD)

G3(MP2)	DMMP	sarin (GB)	soman (GD)
ionization potential (IP) (eV)	10.7 (10.0)[a]	9.82	10.2
fluoride affinity (FA) (kJ mol^{-1})	118	152	156
proton affinity (PA) (kJ mol^{-1})	898 (902)[b] (911)[c]	857	864

[a] Experimental value from NIST Webbook.[34] [b] Experimental value from Tabrizchi and Shooshari.[14] [c] Unpublished value from Stone. See ref 15.

H_3O^+ is a common CIMS reagent ion, which has been found to react with DMMP exclusively by nondissociative proton transfer. Thus, the molecule remains intact, potentially satisfying the selectivity requirement for chemical ionization. The proton affinities listed in Tables 1 and 3 show that this reaction is over 200 kJ mol^{-1} exothermic. Despite this large exothermicity, no fragmentation has been observed. These data agree with the room temperature experiments of both Cordell et al. who used a chemical ionization reaction time-of-flight mass spectrometer (CIR-TOF-MS) at 4.5 Torr[22] and Chatterjee et al. who used a selected ion flow drift tube (SIFDT) at 0.5−1.0 Torr.[19] The current SIFT rate constant is close to the collision rate constant value, but it is 4 times greater than the previous SIFDT experimental value.[19] The current experiments use a very dilute mixture of DMMP in helium that reacts with the selected reactant ion for a fixed reaction time while the flow of the mixture is varied. The Chatterjee et al. experiments, on the other hand, have used a neat DMMP sample cooled in a dry ice bath at a concentration determined by measuring the pressure of DMMP with a capacitance manometer.[19] Using the neat vapor from a low vapor pressure liquid can result in a loss of sample to the inlet line walls for reagents that are "sticky". Thus, the actual concentration in the SIFDT experiments might have been less than has been assumed, meaning the measured rate constants of Johnsen and co-workers may have been in error. The vapor pressure added to the mixtures in the current experiments has been kept at or below the room temperature vapor pressure of DMMP, and the helium in the dilute mixture helps to flush the inlet line between data points to minimize these effects. It is unknown whether neutral dimers are produced in the reactant gas sample that could affect the measured rate constant, but previous experience indicates that is rarely, if ever, a problem.

In addition, water clusters are often present when H_3O^+ is used as a CIMS reagent ion. Therefore, the reactions of $H_3O^+(H_2O)_n$ for $n = 1$ and 2 with DMMP have also been studied and are found to be similarly rapid. Each cluster has been produced separately and cleanly in the flow tube by tuning the upstream quadrupole mass filter to inject the cluster with size $n + 2$ and adjusting the injection conditions to produce only the desired ion. The reaction enthalpies for proton transfer from these two cluster ions have been calculated using the sum of the PA difference between DMMP and H_2O and the average bond dissociation energies for removing n water molecules.[34]

The first hydrate, $n = 1$, produces exclusively protonated DMMP, given as $[H_3CP(O)(OCH_3)_2]H^+$. This reactivity is expected because the bond strength of the first water molecule with H_3O^+ is considerably less than the proton affinity difference between H_2O and DMMP.[35] The second hydrate, $n = 2$, produces $[H_3CPO(OCH_3)_2]H^+$ in ∼3/4 of the reactions, with the other 1/4 producing the first hydrate of protonated DMMP as seen in Table 1. The energetics are such that production of protonated DMMP is approximately thermoneutral for $H_3O^+(H_2O)_2$.[35] This observation may indicate that the water molecule is more weakly bound to protonated DMMP, which is consistent with the estimated binding energy of 58 kJ mol^{-1} determined by Ewing et al.[16] They have also found that the first hydrate of protonated DMMP can be observed in their IMS study of proton-bound dimers at 298 K, but this cluster is observed at 340 K only at higher water concentrations in the instrument and has not been observed above 488 K. The

experiments of Cordell et al. in a CIR-TOF-MS further support this view, where only the proton transfer product with DMMP has been observed in the reaction with H_3O^+ in humid air. Their instrument uses a drift field in the reactor designed to reduce clustering at the higher operating pressure, further implying that H_2O does not strongly bind to protonated DMMP.[22] Such weakly bound hydrates can also thermally decompose at room temperature in the SIFT through collisions with the helium buffer, making it difficult to ascertain whether the measured branching ratio completely reflects the nascent branching ratio.[36] Temperature dependence studies can sometimes shed light on the mechanism; however, those experiments are beyond the scope of this survey.

Two other common proton transfer reagents, $(CH_3)_2COH^+$ and NH_4^+, also react exclusively by nondissociative proton transfer, indicating that the PA of DMMP is greater than that of ammonia (853 kJ mol^{-1}). This observation is consistent with the calculated PA of 898 kJ mol^{-1} for DMMP presented in Table 3, which is in excellent agreement with the experimental value of 902 kJ mol^{-1} from Tabrizchi and Shooshari[14] and in decent agreement with the unpublished value from Stone of 911 kJ mol^{-1}.[15] The absence of any dissociative proton transfer indicates that these two ions would be good CIMS reagent ions. H_3O^+ is known to react with many trace gases;[37] therefore, $(CH_3)_2COH^+$ and NH_4^+ will be more selective than H_3O^+ because of the higher proton affinities of their neutral precursors.

To set better limits on the proton affinity of DMMP, we have also chosen to study species with higher proton affinities, for example, protonated methylamine ($CH_3NH_3^+$) and triethylamine ($(C_2H_5)_3NH^+$). While both ions react rapidly, the mechanism changes to clustering. Proton transfer is calculated to be essentially thermoneutral from $CH_3NH_3^+$ to DMMP and to be clearly endothermic from $(C_2H_5)_3NH^+$. Thus, the absence of proton transfer intimates that the proton affinity of DMMP is at least as large as the calculated value in Table 3. Highly exothermic proton transfer reactions will not typically generate stable association products, but the observed clustering reactions probably indicate that most, if not all, of the reactions involving protonated species proceed through a long-lived complex.

Two CIMS agents that frequently react by charge transfer have also been studied, O_2^+ and NO^+. These species have been chosen because they are currently used in two of the commercial ion reactors based on the SIFT method.[20] NO^+ reacts at around 70% of the collision rate constant and only forms an association product, which suggests that the IP of DMMP is greater than that of NO (9.26 eV). The calculated IP (10.7 eV) and measured IP (10.0)[34] of DMMP shown in Table 3 concur with this observation and are in good agreement with appearance energy of 10.48 eV for the DMMP cation at $m/z = 124$ amu seen in previous EI experiments.[11] Both Cordell et al.[22] and Chatterjee et al.[19] have also only seen the association product from reaction of DMMP with NO^+. In the more energetic reaction with O_2^+, the rate constant is essentially equal to the collisional value to create the DMMP cation at $m/z = 124$ amu in around one-half of the collisions. This reaction is 1.4−2.1 eV exothermic, depending on the IP value of DMMP. Chatterjee et al. have also found this product to be one of the two major product ions in a SIFDT, but this product accounts for 34% of their product ions, with the rest appearing as lower mass product ions at thermal energies with a strong dependence on the center-of-mass kinetic energy.[19]

A minor product ion channel at 125 amu giving $OPO(OCH_3)_2^+$ from exchange of an O for the CH_3 group has been observed in the SIFT with the O_2^+ reaction. As seen in Table 1, exchange of an O atom for the methyl group to produce a CH_3O fragment and $OP(O)(OCH_3)_2^+$ is 180 kJ mol^{-1} exothermic. In contrast, Johnsen and co-workers have not reported seeing this product channel. They have also shown that the DMMP product ions can undergo rapid secondary reactions with neutral DMMP. The 125 amu product ion may undergo rapid secondary chemistry in the SIFDT experiments, which have been done using neat vapor samples of DMMP at larger concentrations than used currently.[19] Memory effects from having residual concentrations of DMMP present may contribute to secondary chemistry, depleting the minor 125 amu channel in the SIFDT measurements.

On the other hand, the mass spectrum of Cordell et al. for the reaction of O_2^+ with DMMP using CIR-TOF-MS shows an overwhelming peak at $m/z = 125$ amu that they attribute to reaction from a large H_3O^+ impurity. They only see a small peak at 124 amu, which they argue is because of limited reactivity of O_2^+ with DMMP.[22] Further examination of their mass spectrum shows additional peaks of size comparable to the 124 amu peak at the m/z ratios of the peaks observed in the current SIFT measurements outlined in Table 1. It is possible that the formation of the 125 amu $OPO(OCH_3)_2^+$ ion may rapidly be converted to the more abundant product ions observed in the SIFT experiments, which are conducted at 10 times lower pressure than the CIR-TOF-MS experiments as discussed below. Therefore, this product ion might be favored at the higher operating pressure of the CIR-TOF-MS, but its presence might be obscured by the H_3O^+ impurity in their measurements.[22]

The other main product seen in the SIFT experiments with O_2^+ is $OP(O)(OCH_3)^+$ at $m/z = 94$ amu, in agreement with the SIFDT results.[19] The CH_3O product fragment formed during the creation of the 125 amu product could then abstract one of the CH_3O groups to form CH_3OOCH_3 and $OP(O)(OCH_3)^+$, possibly in a sequential-type reaction that is overall 283 kJ mol^{-1} exothermic. As shown in Table 1, three other 94 amu product ion isomers can be formed exothermically from the net loss of CH_2O with different combinations of H migration and rearrangement.

A number of minor ions also occur essentially at our detection limit and are subsequently listed as limits in Table 1. Chatterjee et al.[19] have also observed the minor product ions at $m/z = 79$ and 109 amu seen in the current experiments, but they have found larger branching fractions for these two product ions, again potentially from secondary chemistry as discussed above. Forming product ions at 79 amu with either a P−H or a P−O−H bond is exothermic when accompanied by loss of CH_2O and formation of CH_3O_2, consistent with the speculation by Chatterjee et al.[19] that complex ion−molecule chemistry could be involved in generating this product given that the appearance energy in the EI experiments[11] exceeds the recombination energy of O_2^+. Observation of a stable product ion at 125 amu supports this view because it requires breaking bonds to incorporate the O atom into DMMP with subsequent CH_3 loss. However, generating the $P(O)(OCH_3)_2^+$ product at 109 amu via dissociative charge transfer with CH_3 loss is 88 kJ mol^{-1} exothermic. Nevertheless, even under the optimal mass selection and injection conditions for O_2^+, it is possible that some of these minor ions may be attributed to trace reactant ions such as O^+ or H_3O^+ present at the $\leq$1−2% level in the flow tube that cannot be completely be avoided. Further speculation as to the reaction mechanism producing the observed fragment ions is secondary to the goal of finding ionic signatures for use in CIMS detection schemes and is beyond the scope of the current study.

O^+ has a recombination energy 1.5 eV higher than that for O_2^+. Nondissociative charge transfer has not been seen in the reactions of DMMP with O^+, consistent with the SIFDT data of Johnsen and co-workers.[19] A minor 125 amu has also been observed with O^+ that again has not been seen in the previous SIFDT studies.[19] In both the current studies and the earlier SIFDT work,[19] the most abundant ionic product is at $m/z = 79$ amu. Forming either $HOPOCH_3^+$ or $HP(O)OCH_3^+$ is exothermic if the resulting fragments are CH_2O and CH_3. Product ions at both $m/z = 94$ and 93 amu have been observed in the SIFT in about a 4:1 ratio, consistent with the thermal energy data of Johnsen and co-workers.[19] Exothermic reaction channels for all four 94 amu isomers proposed for the O_2^+ reaction can also be found for the O^+ reaction with DMMP as shown in Table 1. Three different isomers of the 93 amu product ion also can be formed exothermically that reflect which carbon bonds in DMMP are broken. In addition, loss of a single $-CH_3$ group from either the phosphorus or the $-OCH_3$ group occurs 14% of the time and is 211 and 299 kJ mol^{-1} exothermic, respectively, especially if CH_3O is formed with the latter channel.

b. Negative Ion Reactions. Negative ions have been found to be much less reactive with DMMP. For SF_5^-, SF_6^-, and CO_3^-, no reaction has been observed, giving an upper limit to the rate constant of $k < 10^{-11}$ cm^3 s^{-1}. The lack of fluoride transfer to make $DMMPF^-$ is consistent with the calculated FA values as discussed later. Because SF_6^- transfers F^- as readily as most F^- transfer reagents, no further studies on potential F^- transfer agents have been performed. NO_3^- does not react with DMMP either, again having an upper limit to the rate constant of $k < 10^{-11}$ cm^3 s^{-1}. Alternatively, NO_2^- reacts slowly to form a cluster with DMMP through a three-body association process. While the bimolecular rate constant measured at 0.4 Torr is too small to be useful, it may become larger with increasing pressure. However, this reaction is probably not suitable for use as a CIMS detection scheme and will not be discussed further.

While fluoride attachment does not occur, the F^- ion reacts rapidly at 75% of the collisional limit, forming two reactive product channels: abstraction of CH_3 to form CH_3F and substitution of F for a CH_3OH. These two product channels have also been observed by Lum and Grabowski in a flowing afterflow study of negative ion reactions with DMMP.[18] The SIFT branching ratios are in excellent agreement with their results that show CH_3 abstraction is the dominant channel. The minor channel forming $FP(O)(OCH_3)(CH_2)^-$ is 79 kJ mol^{-1} endothermic. However, the numerous vibrational modes of DMMP provide just enough rovibrational energy to allow this pathway to be energetically possible. This is consistent with its small branching ratio. Lum and Grabowski propose competing reaction pathways where CH_3F is created via an S_N2 nucleophilic substitution at the C−O bond of one of the $-OCH_3$ groups in DMMP. This pathway predominates when the primary proton transfer channel seen with other anions becomes endothermic as with F^-. Formation of an F^-•DMMP complex with subsequent attack at the phosphorus through an "in-line" displacement that involves a pentacoordinate transition structure can remove CH_3O^- within the complex, which can then deprotonate the phosphorus methyl group to form CH_3OH.[18] Generating $H_3CP(O)O(OCH_3)^-$ and $FP(O)(OCH_3)(CH_2)^-$ product ions at 109 and 111 amu, respectively, could provide a selective reaction mechanism; however, F^- is not commonly used in present CIMS instrumentation.

Both O^- and O_2^- react rapidly with DMMP. O^- reacts mostly by H_2^+ abstraction to form H_2O as is commonly seen with other O^- reactions.[38] The lowest energy pathway found through the G3(MP2) calculations involves removing one H from the phosphorus methyl group and the other H from an adjacent $-OCH_3$ group and is 155 kJ mol^{-1} exothermic. However, it is also exothermic to remove the H_2^+ entirely from the phosphorus $-CH_3$ group or one of the $-OCH_3$ groups, as well as removing one H from each of the two $-OCH_3$ groups. Production of CH_3O through the O^- reaction by removing either the phosphorus $-CH_3$ group or an $-OCH_3$ methyl group to create the 109 amu product ion is exothermic and occurs in 18% of the reactions. This product ion is the dominant product in the O_2^- reaction (98%). The most exothermic pathway found through the G3(MP2) calculations for the O_2^- reaction (124 kJ mol^{-1}) involves abstracting a methyl from one of the $-OCH_3$ groups to generate CH_3O_2. However, it is also exothermic to remove the phosphorus $-CH_3$ group, but this pathway requires the formation of CH_2O and OH fragments, which would be a more complicated mechanism. An association reaction channel with O_2^- is only a minor pathway. O_2^- is sometimes used in ion mobility spectrometry (IMS) as part of negative ion reaction schemes.[39] As IMS also relies on ion chemistry for detection, the O_2^- reactant ion should be considered as a potential CIMS agent.

c. Ion Energetics Calculations. The ionization potentials, fluoride, and proton affinities of DMMP, sarin, and soman calculated using G3(MP2) theory are given in Table 3. The proton attaches preferentially to the oxygen on the P═O group in all three compounds, while the F^- binds to the central P atom in all three species. The charge distributions have the most positive charge centered on the P, while the negative charge is highest on the oxygen atoms, of which the P═O is most accessible. The similarity among the calculated energetics shown in Table 3 reflects this common arrangement, with the differences in the −OR groups accounting for the differences in the values found. As discussed above, the calculated PA is in very good agreement with literature values,[14,15] as is the calculated IP as compared to the experimental values of 10.0 eV[34] and the appearance energy of ∼10.5 eV.[11] Furthermore, the minimum energy structures for the observed positive ion fragments reflect which bond is cleaved in the dissociation process.

Discussion

The goal of the present study is to determine likely candidates for chemical ionization reagents for sarin (GB) and soman (GD) detection. Figure 1 shows the structures of DMMP, sarin, and soman. Each molecule has a central P atom with a methyl group and P−O double bond. Additionally, each molecule has one RO group attached, with sarin and soman differing only by the identity of R. The main difference between the DMMP surrogate and the CW agents is that the fourth constituent attached to the central P atom is F in the CW agents and CH_3O in DMMP. Therefore, the surrogate and CW agents should display similar reactivity patterns, unless the P−F reactivity dominates. Studies of the reactivity of H_3O^+ with sarin in both dry and humid air by Cordell et al. have not shown any contributions from an F^- abstraction channel to give HF, indicating that this assumption is reasonable.[22] Differences in the reaction thermodynamics for DMMP versus the GX compounds should be adequately handled by our calculations of the various ion energetic properties.

The positive ion results show that DMMP clusters rapidly to NO^+, leaving the DMMP intact; therefore, it should be detected both sensitively and selectively using NO^+ reactions. While the IPs of sarin and soman are less than that of DMMP, they are still greater than the IP of NO and the chemistry should be

similar. Indeed, a recent conference report on detection of sarin using the SYFT Technologies commercially produced selected ion flow tube instrument has shown that NO^+ indeed clusters rapidly, confirming the present approach.[21] O_2^+, which is also used in the SYFT instrument, reacts with DMMP to produce the DMMP cation in ~50% of collisions. The calculated IP of sarin is about 1 eV lower than that for DMMP. Thus, the charge transfer reaction of O_2^+ with sarin will be more exothermic; that is, the reaction energetics should be closer to those involving O^+, which did not form any sarin cation.[21] Consequently, extrapolation of the present results on DMMP to sarin indicates that nondissociative charge transfer between O_2^+ and sarin is probably a small reaction channel. This assumption has again been confirmed in an unpublished study using the SYFT Technologies instrument, where a sarin cation peak is absent, alternatively resulting in a cation peak for methyl loss from sarin. The sensitivity has been further reduced because of the formation of several additional product ions.[21]

The third ion currently in use in the commercial instruments is H_3O^+.[20] The current DMMP results show that this ion should be a sensitive and selective reagent ion for GX series detection because only rapid nondissociative proton transfer occurs to give a single product ion, in agreement with the results of Cordell et al.[22] Again, the unpublished SYFT results also confirm that H_3O^+ reacts with sarin rapidly by proton transfer,[21] in agreement with the results of Cordell et al.[22] Thus, our results on the DMMP surrogate are completely compatible with the previous studies.[21,22] Each of three cations discussed produces a unique product ion and they can be rapidly interchanged in an instrument; therefore, the combination should lead to a situation where false positives may be avoided. Detection limits in the SYFT Technologies experiments have been shown to be on the order of 400 pptV, but those studies used a first generation version of the commercial instrument.[21] A second generation model of that instrument is much more sensitive. It remains to be seen whether atmospheric impurities at small concentrations will produce background signals.

While the detection limits of the commercial instruments are quite good,[20] research grade CIMS instruments in use for atmospheric chemistry have higher sensitivity and often greater selectivity.[40] The increased sensitivity is achieved, in part, by larger pumps and bigger instrument sizes that produce more favorable reaction conditions for measuring smaller concentrations. The enhanced selectivity is often achieved by using negative ion reactions. Fluoride transfer is often very selective, if the reaction is exothermic. One of the best fluoride transfer agents is SF_6^-, which has a SF_5-F^- bond strength slightly over 200 kJ mol^{-1}.[41] The present experiments show that neither SF_6^-, nor SF_5^-, reacts with DMMP. The FA calculations show that DMMP has a small fluoride affinity; thus, the lack of reactivity is not surprising. The experiments with F^- ions show that F^- undergoes substitution, rather than simply attaching to DMMP, and the reaction is endothermic. Sarin and soman have calculated fluoride affinities considerably larger than that of DMMP, but the FA is still less than that for SF_5. However, the calculated values have enough uncertainty that F^- transfer from SF_6^- to the CWAs cannot be completely ruled out. Thus, fluoride transfer experiments on the live warfare agents may be worthwhile.

Nevertheless, one possible negative ion CIMS reagent is O_2^-, which can be readily produced when high pressure atmospheric gas is ionized. O_2^- has been used as a chemical ionization reagent in both CIMS instruments and in more portable ion mobility spectrometers (IMS).[39] Our results show that a rapid reaction proceeds through a net loss of a $-CH_3$ group from DMMP, possibly from the central phosphorus. As the agents have a similar methyl group, analogous chemistry may be expected and should probably be selective. Both O^- and F^- react with DMMP, but these two ions are not easily used in present CIMS and IMS instrumentation.

Conclusions

We have studied the reactions of an array of ions with the GX-series structural surrogate, dimethyl methylphosphonate (DMMP), at 298 K in a SIFT to find good candidates for CIMS or IMS detection of sarin and soman. The experimental results are accompanied by G3(MP2) calculations of the ionic properties of DMMP, sarin, and soman so that the data for the surrogate chemistry can be extrapolated to reactions with the chemical weapons agents themselves. Several candidate reagent ions have been identified, including H_3O^+, NO^+, and O_2^-, while many other candidate ions have been ruled out. The predictions derived from a combination of experiment and theory are credible based upon comparisons to results for the detection of sarin in commercial CIMS-type instruments.[21,22]

Acknowledgment. We would like to thank Jim Buchanan at the U.S. Army Edgewood Chemical Biological Center (ECBC) for experimental vapor pressure data for DMMP. We would like to thank John Williamson and Paul Mundis for their technical support. This project is supported by the Army Research Office (ARO) under the JSTO program in Chemical and Biological Defense (JSTO-CBD) and the Molecular Dynamics program at Air Force Office of Scientific Research (AFOSR). A.J.M. and T.M.M. are supported under Boston College contract number FA8718-04-C-0006. The soman calculations have been performed on the Scorpio Linux cluster at Boston College.

References and Notes

(1) *NRC Monitoring at Chemical Agent Disposal Facilities*; National Academy of Sciences: Washington, DC, 2005.
(2) Eisele, F. L.; Tanner, D. J. *J. Geophys. Res.* **1993**, *98*, 9001.
(3) Ballenthin, J. O.; Thorn, W. F.; Miller, T. M.; Viggiano, A. A.; Hunton, D. E.; Koike, M.; Kondo, Y.; Takegawa, N.; Irie, H.; Ikeda, H. *J. Geophys. Res.* **2003**, *108*, 4188.
(4) Hunton, D. E.; Ballenthin, J. O.; Borghetti, J. F.; Federico, G. S.; Miller, T. M.; Thorn, W. F.; Viggiano, A. A.; Anderson, B. E.; Cofer, W. R.; McDougal, D. S.; Wey, C. C. *J. Geophys. Res.* **2000**, *105*, 26841.
(5) Mauldin, R. L., III; Tanner, D. J.; Eisele, F. L. *J. Geophys. Res.* **1998**, *103*, 3361.
(6) Marcy, T. P.; Gao, R. S.; Northway, M. J.; Popp, P. J.; Stark, H.; Fahey, D. W. *Int. J. Mass Spectrom.* **2005**, *243*, 63.
(7) Schneider, J.; Burger, V.; Arnold, F. *J. Geophys. Res.* **1997**, *102*, 25.
(8) Chen, G.; Huey, L. G.; Trainer, M.; Nicks, D.; Corbett, J.; Ryerson, T.; Parrish, D.; Neuman, J. A.; Nowak, J.; Tanner, D.; Holloway, J.; Brock, C.; Crawford, J.; Olson, J. R.; Sullivan, A.; Weber, R.; Schauffler, S.; Donnelly, S.; Atlas, E.; Roberts, J.; Flocke, F.; Hübler, G.; Fehsenfeld, F. *J. Geophys. Res.* **2005**, *110*, D10S90.
(9) Tremmel, H. G.; Schlager, H.; Konopka, P.; Schulte, P.; Arnold, F.; Klemm, M.; Droste-Franke, B. *J. Geophys. Res.* **1998**, *103*, 10803.
(10) Midey, A. J.; Miller, T. M.; Viggiano, A. A. *J. Phys. Chem. A* **2008**, *112*, 10250.
(11) Bafus, D. A.; Gallegos, E. J.; Kiser, R. W. *J. Phys. Chem.* **1966**, *70*, 2614.
(12) Chen, H.; Zheng, X.; Cooks, R. G. *J. Am. Soc. Mass Spectrom.* **2003**, *14*, 182.
(13) Meurer, E. C.; Chen, H.; Riter, L. S.; Cooks, R. G. *J. Am. Soc. Mass Spectrom.* **2004**, *15*, 398.
(14) Tabrizchi, M.; Shooshtari, S. *J. Chem. Thermodyn.* **2003**, *35*, 863.
(15) Ewing, R. G.; Eiceman, G. A.; Stone, J. A. *Int. J. Mass Spectrom.* **1999**, *193*, 57.
(16) Ewing, R. G.; Eiceman, G. A.; Harden, C. S.; Stone, J. A. *Int. J. Mass Spectrom.* **2006**, *76*, 255–256.

(17) Eiceman, G. A.; Wang, Y.-F.; Garcia-Gonzalez, L.; Harden, C. S.; Shoff, D. B. *Anal. Chim. Acta* **1995**, *306*, 21.
(18) Lum, R. C.; Grabowski, J. J. *J. Am. Chem. Soc.* **1993**, *115*, 7823.
(19) Chatterjee, B. K.; Tosh, R.; Johnsen, R. *Int. J. Mass Spectrom. Ion Processes* **1991**, *103*, 81.
(20) Examples: http://www.ptrms.com, http://www.syft.com, and http://www.transpectra.com.
(21) Francis, G. J.; Langford, V. S.; Milligan, D. B.; McEwan, M. J. Real time detection and quantification of dangerous substances in air without sample preparation using SIFT-MS; 56th ASMS Conference on Mass Spectrometry and Allied Topics, Denver, 2008.
(22) Cordell, R. L.; Willis, K. A.; Wyche, K. P.; Blake, R. S.; Ellis, A. M.; Monks, P. S. *Anal. Chem.* **2007**, *79*, 8359.
(23) Viggiano, A. A.; Morris, R. A.; Dale, F.; Paulson, J. F.; Giles, K.; Smith, D.; Su, T. *J. Chem. Phys.* **1990**, *93*, 1149.
(24) Curtiss, L. A.; Redfern, P. C.; Raghavachari, K.; Rassolov, V.; Pople, J. A. *J. Chem. Phys.* **1999**, *110*, 4703.
(25) Frisch, M. J.; Trucks, G. W.; Schlegel, H. B.; Scuseria, G. E.; Robb, M. A.; Cheeseman, J. A., Jr.; Montgomery, J.; Vreven, T.; Kudin, K. N.; Burant, J. C.; Millam, J. M.; Iyengar, S. S.; Tomasi, J.; Barone, V.; Mennucci, B.; Cossi, M.; Scalmani, G.; Rega, N.; Petersson, G. A.; Nakatsuji, H.; Hada, M.; Ehara, M.; Toyota, K.; Fukuda, R.; Hasegawa, J.; Ishida, M.; Nakajima, T.; Honda, Y.; Kitao, O.; Nakai, H.; Klene, M.; Li, X.; Knox, J. E.; Hratchian, H. P.; Cross, J. B.; Adamo, C.; Jaramillo, J.; Gomperts, R.; Stratmann, R. E.; Yazyev, O.; Austin, A. J.; Cammi, R.; Pomelli, C.; Ochterski, J. W.; Ayala, P. Y.; Morokuma, K.; Voth, G. A.; Salvador, P.; Dannenberg, J. J.; Zakrzewski, V. G.; Dapprich, S.; Daniels, A. D.; Strain, M. C.; Farkas, O.; Malick, D. K.; Rabuck, A. D.; Raghavachari, K.; Foresman, J. B.; Ortiz, J. V.; Cui, Q.; Baboul, A. G.; Clifford, S.; Cioslowski, J.; Stefanov, B. B.; Liu, G.; Liashenko, A.; Piskorz, P.; Komaromi, I.; Martin, R. L.; Fox, D. J.; Keith, T.; Al-Laham, M. A.; Peng, C. Y.; Nanayakkara, A.; Challacombe, M.; Gill, P. M. W.; Johnson, B.; Chen, W.; Wong, M. W.; Gonzalez, C.; Pople, J. A. *Gaussian 03W*, revision C.02; Gaussian, Inc.: Pittsburgh, PA, 2003.
(26) Su, T. *J. Chem. Phys.* **1988**, *89*, 5355.
(27) Su, T.; Chesnavich, W. J. *J. Chem. Phys.* **1982**, *76*, 5183.
(28) Miller, K. J. *J. Am. Chem. Soc.* **1990**, *112*, 8533.
(29) Bosque, R.; Sales, J. *J. Chem. Inf. Comput. Sci.* **2002**, *42*, 1154.
(30) Kosolapoff, G. M. *J. Chem. Soc.* **1954**, 3222.
(31) Barnes, A. J.; Lomax, S.; Van der Veken, B. J. *J. Mol. Struct.* **1983**, *99*, 137.
(32) Florin, J.; Trajbl, M.; Warshel, A. *J. Am. Chem. Soc.* **1998**, *120*, 7959.
(33) Lewars, E. *Computational Chemistry: Introduction to the Theory and Applications of Molecular and Quantum Mechanics*; Kluwer Academic Publishers: Norwell, MA, 2003.
(34) *NIST Chemistry WebBook, NIST Standard Reference Database No. 69*; Linstrom, P. J., Mallard, W. G., Eds.; National Institutes of Standards and Technology: Gaithersburg, MD, 2007; http://webbook.nist.gov.
(35) Keesee, R. G.; Castleman, A. W., Jr. *J. Phys. Chem. Ref. Data* **1986**, *15*, 1011.
(36) Viggiano, A. A.; Arnold, S. T.; Morris, R. A. *Int. Rev. Phys. Chem.* **1998**, *17*, 147.
(37) Conference Proceedings; 3rd International Conference on Proton Transfer Reaction Mass Spectrometry and its Applications, Obergurgl, Austria, 2007.
(38) Lee, J.; Grabowski, J. J. *Chem. Rev.* **1992**, *92*, 1611.
(39) Eiceman, G. A.; Karpas, Z. *Ion Mobility Spectrometry*; CRC Press: Boca Raton, FL, 1993.
(40) Viggiano, A. A. *Mass Spectrom. Rev.* **1993**, *12*, 115.
(41) Miller, T. M.; Arnold, S. T.; Viggiano, A. A. *Int. J. Mass Spectrom.* **2003**, *227*, 413.

JP900614A